

Performance gains in the D-Wave Advantage2 system at the 4,400-qubit scale

WHITEPAPER

Summary

We benchmark the performance of the Advantage2™ quantum-processing unit (QPU), a 4,400+ annealing quantum computer interconnected in the Zephyr™ topology, against a previous-generation QPU on the optimization task of solving 3D-lattice spin glasses of tunable precision. We present performance results that highlight the benefits of our latest fabrication upgrade, which yields significant improvements in solution quality over a range of test scenarios. In some cases, the Advantage2 system produces better quality solutions using anneal times that are several orders of magnitude faster than those used on the previous-generation Advantage™ system.

1 Introduction

In May 2025, D-Wave released our largest Advantage2 system, a Zephyr-12 (Z_{12}) QPU featuring over 4,400 qubits and over 40,000 couplers. The Zephyr topology provides 20-way qubit connectivity, a step up from the 15-way connectivity of the Pegasus™ topology found on Advantage systems. Boothby et al. [1] show how this upgraded connectivity allows embedding larger and more interconnected problems than before. Previous work [2] illustrates performance benefits involving more compact embeddings on an Advantage2 system. Here we focus on performance differences due to recent additional improvements in the design and fabrication of our quantum annealing computers.

The Advantage2 system at the 4,400-qubit scale features three major technology upgrades with respect to the previous Advantage system: energy scale, coherence time, and lower noise.

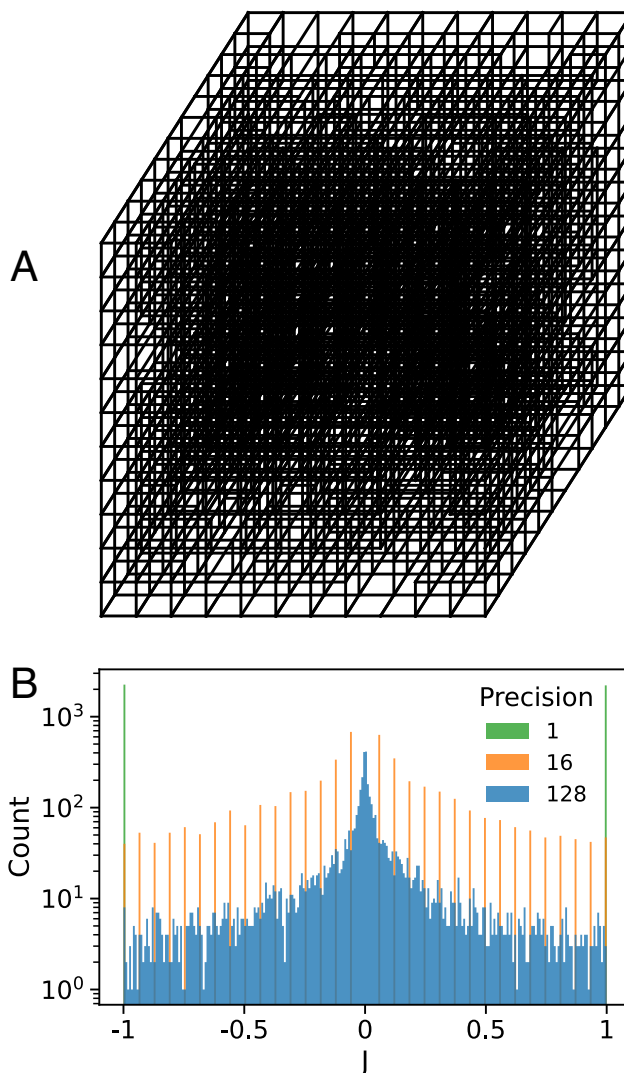


Figure 1: (A) $12 \times 12 \times 12$ lattice with 1,650 nodes and 4,461 edges that embeds on both Advantage and Advantage2 systems with two-qubit chains. (B) Histogram of quadratic weights in three instances of the problem class $power-r$ with precision $r = 1, 16, 128$.

- **40% higher energy scales.** A quantum annealing computer solves an optimization problem by mapping the objective function to an energy landscape. Then, it uses an algorithm implemented in hardware and software to find low-energy and minimum solutions in the landscape. Higher energy scales means greater energy separation between high-quality solutions and lower-quality ones, driving results closer to optimal. Quantum dynamics are also accelerated proportionately.
- **2× longer coherence time.** Longer coherence time means that the QPU can perform undisturbed coherent Hamiltonian evolution for longer time intervals throughout the annealing protocol. This improves the effectiveness of the quantum annealing algorithm.
- **4× lower noise.** Noise translates into imprecision when representing problem weights in an annealing quantum computer, resulting in the QPU solving a problem slightly different from the one intended. Lower noise allows improved resolution of the ground state and energy gaps, supporting more accurate high precision programming.

In this paper, we use the *fast anneal* protocol to illustrate the performance of two generations of QPUs across a wide range of annealing times. In fast anneals, the transverse and longitudinal fields follow a slightly different trajectory than in the standard protocol [3, 4], and allow the user to anneal for as short as 5 ns (the minimum anneal time of the standard protocol is 500 ns). Nanosecond anneals are fast enough to avoid thermal excitations from the environment, allowing for effectively undisturbed coherent evolution of the Hamiltonian. Fast anneals have provided a number of results agreeing with coherent theory in the fields of quantum optimization [5] and quantum simulation [6, 7].

We solve the largest 3D lattice that embeds on both Advantage and Advantage2 systems — a $12 \times 12 \times 12$ cube with 1,650 nodes and 4,461 edges shown in Fig. 1A. This graph embeds on both QPUs with two-qubit chains.

The 3D-structured problems are random spin glasses of tunable precision r , using a weighting scheme called *power- r* that promotes the frequency of small weights, see Fig. 1B. This problem class consists of Ising models with linear fields h set to zero, and quadratic interactions J sampled from the integer range (skipping zero) $\{-r, -r+1, \dots, -1, 1, \dots, r-1, r\}$ with power-law probability $P(J) \propto 1/|J|$. When $r = 1$,

the problem reduces to the familiar $J \in \{-1, +1\}$ spin-glass problem. Weights are fit into the QPU J -range $[-2, 1]$ by dividing them by r . By increasing the problem parameter r , one increases the precision requirements of the QPU when performing the quantum annealing protocol.

2 Results

Fig. 2 characterizes the performance of both generations of quantum annealers when solving 3D instances of varying levels of precision $r = 1, 16, 128$. Relative error is defined as the relative energy distance of a given solution from the ground state energy: $RE = (E_{\text{sol}} - E_{\text{gs}}) / |E_{\text{gs}}|$. Smaller RE corresponds to better (lower-energy) solutions. Boxplots report sample statistics from 1001 anneals on a single QPU programming per problem, over ensembles of 101 problems per class. Light boxplots show the distribution of sample medians, representing the overall sampleset quality. Bold boxplots show the distribution of sample minima, ie. the best solutions obtained from each call to the QPU.

The three panels of Fig. 2 show that when annealing for the same time length, the Advantage2 system outperforms the Advantage system in both median and minimum sample quality by a well-separated objective gap of 2× to 7×, depending on the length of the anneal. This clear separation is due to the combined effect of higher energy scales, extended coherence and lower noise.

In the shortest annealing times (below ~ 100 ns), we observe a steep descent towards optimality consistent with the findings in [5]. These anneals are fast enough to avoid thermal excitations from the environment, allowing the system to follow the quantum annealing Hamiltonian evolution protocol more closely. This translates to optimization speedups compared to what is possible from classical dynamics. Note that in the Advantage2 QPU, this regime extends further in annealing time, reaching lower relative error, owing to both longer coherence time and larger energy scale in the new generation of QPUs.

At longer annealing times (~ 100 ns to ~ 1 μ s), thermal influence from the environment starts to populate excited states without giving the qubits enough time to equilibrate, halting the steep descent towards optimality. Note that thermal influence is minimized when precision is low (Fig. 2A), or when the energy scale of the QPU is higher (Advantage2)

Advantage system vs Advantage2 system

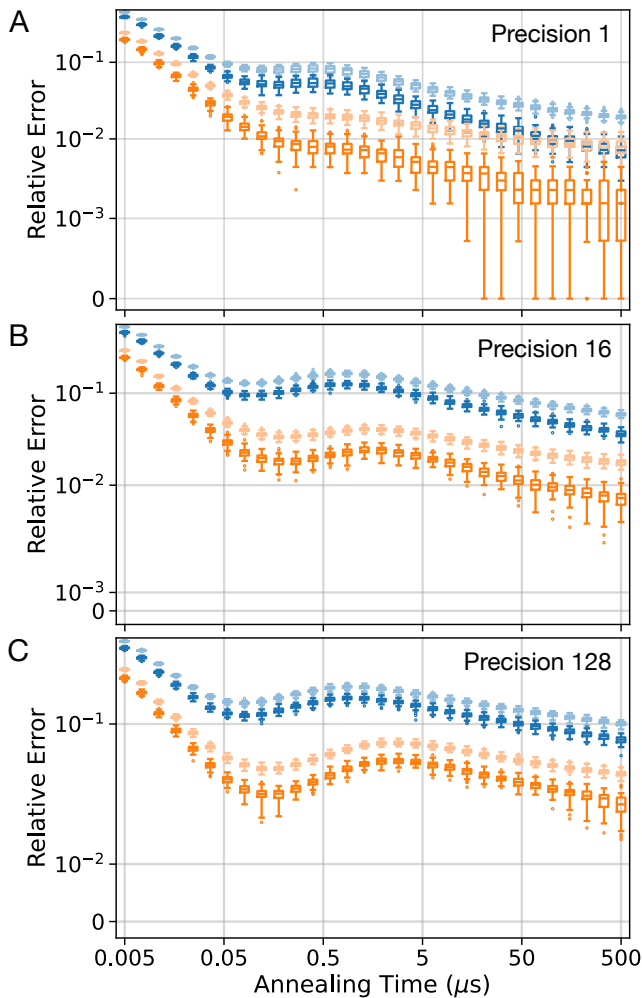


Figure 2: Relative error vs annealing time on problem classes of precision 1, 16, 128. Light-color boxplots show the distribution of sample medians over instances, bold-color boxplots show the distribution of sample minima over instances.

because those increase the excitation barrier.

In the longest time scales (beyond $\sim 1 \mu\text{s}$), solutions continue to improve as the QPUs enter the quasistatic regime with strong environmental coupling [8]. It is in this long-anneal regime that both systems are able to find their best solutions for these instances.

Interestingly, the solution quality obtained with the Advantage system in 500 μs anneals is matched by the Advantage2 system over 1000 \times faster in low-precision instances

$r=1$ (Fig. 2A), and over 10,000 \times faster in higher-precision problems $r=16, 128$ (Fig. 2B,C). In fact, for higher-precision problems, the Advantage system long-anneal performance is surpassed by the Advantage2 system in the coherent regime.

3 Conclusion

This work shows the direct improvements in optimization performance driven by the continuous innovation in our design and fabrication of annealing quantum computers. The Advantage2 system at the 4,400-qubit scale systematically returns better solutions when running for the same annealing time, and can surpass the Advantage system several orders of magnitude faster. These results also highlight the great potential of fast coherent annealing in optimization tasks.

References

- 1 K. Boothby, A. D. King, and J. Raymond, *Zephyr Topology of D-Wave Quantum Processors*, 14-1056A-A (D-Wave Technical Report, 2021).
- 2 *The D-Wave Advantage2 Prototype*, 14-1063A-A (D-Wave Technical Report, 2022).
- 3 *Fast Anneals and Coherent Quantum Annealing*, 14-1074A-A (D-Wave Whitepaper, 2024).
- 4 D.-W. S. Documentation, *Fast-anneal protocol*, https://docs.dwavequantum.com/en/latest/quantum_research/annealing.html#fast-anneal-protocol.
- 5 A. D. King, J. Raymond, T. Lanting, R. Harris, A. Zucca, et al., “Quantum critical dynamics in a 5,000-qubit programmable spin glass,” *Nature* **617**, 61–66 (2023).
- 6 A. D. King, S. Suzuki, J. Raymond, A. Zucca, T. Lanting, et al., “Coherent quantum annealing in a programmable 2,000 qubit ising chain,” *Nature Physics* **18**, 1324–1328 (2022).
- 7 A. D. King, A. Nocera, M. M. Rams, J. Dziarmaga, R. Wiersema, et al., “Beyond-classical computation in quantum simulation,” *Science* **388**, 199–204 (2025), eprint: <https://www.science.org/doi/pdf/10.1126/science.ado6285>.
- 8 M. H. Amin, “Searching for quantum speedup in quasistatic quantum annealers,” *Phys. Rev. A* **92**, 052323 (2015).